

## Intra-arterial infusion of N-isopropyl-p[<sup>123</sup>I]iodoamphetamine for assessing effective blood supply to pulmonary and hepatic neoplasms

Chihoko MIYAZAKI

*Department of Diagnostic Radiology, Sapporo City General Hospital*

The biodistribution and pharmacokinetics of intra-arterially administered N-isopropyl-p[<sup>123</sup>I]iodoamphetamine (<sup>123</sup>I-IMP) were prospectively evaluated in 38 patients with histologically proven pulmonary or hepatic tumors. Intra-arterially infused <sup>123</sup>I-IMP was distributed initially in peripheral tissues in which the blood supply was maintained. Its concentration in malignant neoplasms was demonstrated to be higher than in normal tissues. In pulmonary cancer, the tumor uptake of the administered dose without a tissue attenuation correction (% uptake) of <sup>123</sup>I-IMP at 1–2 min after injection was  $14.7 \pm 5.7\%$  (s.d.). The tumor to normal tissue ratio was  $2.1 \pm 0.7$  in hepatocellular carcinoma and  $1.4 \pm 0.7$  in metastatic tumors. The biodistribution of <sup>123</sup>I-IMP was also compared to that of <sup>99m</sup>Tc-macroaggregated albumin (<sup>99m</sup>Tc-MAA) in 9 cases of hepatic cancer. The distribution of <sup>123</sup>I-IMP resembled that of <sup>99m</sup>Tc-MAA in 5 cases and was different in 4 cases. <sup>123</sup>I-IMP was more concentrated in the tumor than <sup>99m</sup>Tc-MAA.

Intra-arterial infusion scintigraphy with <sup>123</sup>I-IMP seems to provide information on effective blood supply to neoplasms which are targeted in interventional radiology.

**Key words:** tumor blood flow, intra-arterial infusion, N-isopropyl-p[<sup>123</sup>I]iodoamphetamine (<sup>123</sup>I-IMP), interventional radiology

### INTRODUCTION

INTRA-ARTERIAL INFUSION of an anti-tumor chemotherapeutic agent has proven to be effective in the management of primary and metastatic malignant neoplasms. Interventional radiology has come into wide use in this intra-arterial approach. In order to derive the maximal effectiveness by chemotherapy to the target masses, we have to consider several factors: the optimal dose, pharmacokinetics, distribution, and vascular supply of the drug administered intra-arterially. The best way to evaluate intra-cellular drug uptake may be to monitor the biodistribution and pharmacokinetics of the drug labeled with a radionuclide. Positron labeled BCNU and cis-platin have been proposed for the clinical assessment of chemotherapy.<sup>1–3</sup> However, these agents are not available for routine studies.

Radionuclide studies with <sup>99m</sup>Tc-macroaggregated al-

bumin (<sup>99m</sup>Tc-MAA), microspheres and <sup>81m</sup>Kr have been employed for quantifying drug delivery to the target tumor tissue and normal tissue.<sup>4–8</sup> <sup>99m</sup>Tc-MAA perfusion scintigraphy plays a significant role in determining blood perfusion because of its easy availability and appropriate particle size for the first pass capillary blockade. Correlative studies between tumor response and drug distribution via direct measurement of tumor and liver drug levels with <sup>3</sup>H-fluorodeoxyuridine (FUdR) and <sup>99m</sup>Tc-MAA have been reported.<sup>9–11</sup> Also, the prediction of tumor response with both <sup>99m</sup>Tc-MAA and <sup>99m</sup>Tc-sulfur colloid (SC) has been reported.<sup>12,13</sup> Although <sup>99m</sup>Tc-MAA perfusion scintigraphy allows accurate assessment of first-pass blood perfusion to the target masses and surrounding tissues, it is limited as an effective indicator of drug delivery to the extra-cellular space.

N-isopropyl-p[<sup>123</sup>I]amphetamine (<sup>123</sup>I-IMP) was found to be a lipophilic substance and it was cleared from the blood with a greater than 90% extraction fraction on the first pass through the brain when injected into the internal carotid artery.<sup>14,15</sup> Winchell et al. proposed that the initial distribution of <sup>123</sup>I-IMP might be useful for imaging relative regional brain perfusion in humans.<sup>16,17</sup> Kuhl et

Received June 7, 1993, revision accepted December 20, 1993.

For reprint contact: Chihoko Miyazaki, M.D., Department of Diagnostic Radiology, Sapporo City General Hospital, W-9, N-1, Chuo-ku, Sapporo 060, JAPAN.

al., showed that the value of regional cerebral blood flow obtained by the distribution of  $^{123}\text{I}$ -IMP in the brain corresponded closely to the value obtained by the radioactive labeled microsphere method.<sup>18</sup> It is postulated that  $^{123}\text{I}$ -IMP passes through the blood brain barrier and that  $^{123}\text{I}$ -IMP binds to non-specific binding sites, either inside or outside the cell.<sup>19,20</sup> Considering these reports on  $^{123}\text{I}$ -IMP as a freely diffusible and highly extracted tracer for regional cerebral blood flow measurement, the author assumed that the first arterial distribution of  $^{123}\text{I}$ -IMP must reflect the lung and the liver blood perfusion including the neoplasms as well as brain tissues.

The scintigraphic studies concerning the intra-arterial infusion of  $^{123}\text{I}$ -IMP in patients with pulmonary and hepatic neoplasms were designed to investigate the distribution of  $^{123}\text{I}$ -IMP in the lungs and liver to determine the tumor blood flow. In this paper, the first pass distribution, uptake, and change as a function of time in  $^{123}\text{I}$ -IMP in the lungs and the liver were analyzed. Tumor stains on contrast angiograms were compared to those on  $^{123}\text{I}$ -IMP images, and  $^{123}\text{I}$ -IMP and  $^{99\text{m}}\text{Tc}$ -MAA scintigrams were compared in patients with hepatic tumors with respect to the distribution and the intensity of radioactive agents.

## MATERIALS AND METHODS

### Study population

The population studied consisted of 10 patients with pulmonary carcinoma and 28 patients with hepatic tumors (Table 1). All tumors were histologically proven. The patients' ages ranged from 38 to 79 years old. A total of 12 bronchial arterial infusion (BAI) studies with  $^{123}\text{I}$ -IMP were performed in the 10 patients with pulmonary carcinoma immediately after percutaneous bronchial arteriography and interventional chemotherapy. In 12 cases of metastatic hepatic tumors and 2 cases of hepatocellular carcinoma (HCC), hepatic arterial infusion (HAI) studies with  $^{123}\text{I}$ -IMP were performed after percutaneous hepatic arteriography and interventional chemotherapy in which the catheter was placed in the celiac, common hepatic, proper hepatic, right or left hepatic artery. In 5 cases of HCC,  $^{123}\text{I}$ -IMP scintigraphy was carried out before hepatic arterial embolization. HAI studies with both  $^{123}\text{I}$ -IMP and  $^{99\text{m}}\text{Tc}$ -MAA were conducted in the other 9 cases which had undergone operative placement of an hepatic chemotherapy catheter to metastatic tumors. Informed consent was obtained from all patients before the procedures.

### Radionuclide study

Thirty-seven MBq of  $^{123}\text{I}$ -IMP/2 ml was injected slowly through the catheter which was inserted into the bronchial or hepatic arteries and was followed by an infusion of saline solution in 29 patients. In the 9 patients with surgical arterial catheter placements, 37 MBq of  $^{123}\text{I}$ -IMP/2 ml and 185 MBq of  $^{99\text{m}}\text{Tc}$ -MAA/2 ml were introduced

**Table 1** Patient population

Diseases	No. of Patients	Age range
Pulmonary Neoplasm	10	52–72 y.o.
Primary lung cancer	9	
Metastatic breast cancer	1	
Hepatic Neoplasm	28	38–79 y.o.
HCC	7	
Metastatic from	19	
colon	11 (6*)	
stomach	3 (1*)	
bile duct	1 (1*)	
gall bladder	1 (1*)	
lung	1	
pancreas	1	
malignant lymphoma	1	
Benign	2	
regenerative nodule	1	
hemangioma	1	
total	38	

HCC: hepatocellular carcinoma

\*the number indicates combined studies with  $^{123}\text{I}$ -IMP and  $^{99\text{m}}\text{Tc}$ -MAA.

into the hepatic artery through the side port or a subcutaneous reservoir. The  $^{99\text{m}}\text{Tc}$ -MAA study was done within one week after the  $^{123}\text{I}$ -IMP scintigraphy. The studies with  $^{123}\text{I}$ -IMP and  $^{99\text{m}}\text{Tc}$ -MAA were carried out in the supine position with a large-field-of-view gamma camera with a parallel-hole low-energy collimator. Sequential images were obtained every 3 minutes after administration of the radiopharmaceuticals. Data were collected every 30 seconds for 60 minutes by means of a Scintipac 2400 computer.

Before injection, the dose in the syringe was calibrated by the gamma camera under standardized geometry (at 20 cm) for 1 minute. After completion of the procedure, for both the syringe and the catheter, which were pulled out, the remaining radioisotopes were counted in the 29 patients.

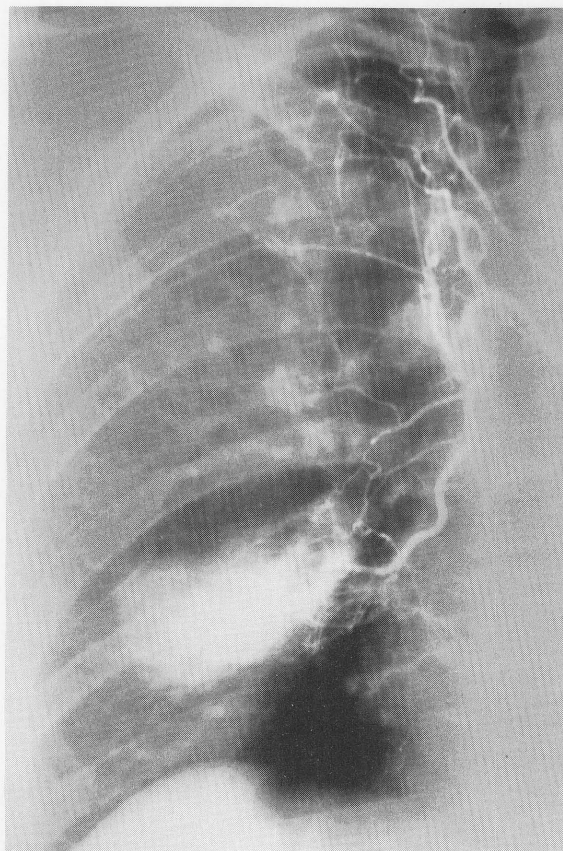
### Data processing

The data were processed according to the following protocol: the region of interest (ROI) of irregular shape was assigned along the increased nodular uptake in the lung or the liver and along the whole lung or liver parenchyma, based on the findings of the chest roentgenogram, CT, liver scintigram and angiogram. Square ROIs ( $5 \times 5$  pixels) were assigned to the normal lung and right lobe of the liver in BAI studies and to the right lung and heart in HAI studies. Time activity curves were generated from all the assigned ROIs.

Percentage uptakes by the whole lung, lung tumor and whole liver of the administered dose were calculated as: [counts of whole lung, lung tumor, or whole liver divided by injection counts]  $\times 100\%$ . They were obtained from 1–2 minute-images after the administration of  $^{123}\text{I}$ -IMP.



A



B

**Fig. 1** A 55-year-old female with pulmonary adenocarcinoma.  $^{123}\text{I}$ -IMP introduced into bronchial artery is distributed at the sites of lung carcinoma (short arrow), pulmonary hilar lymphnode (long arrow) and along the ribs (small arrows) on posterior view at 3 to 6 minutes following i.a. administration of  $^{123}\text{I}$ -IMP (A). Bronchial contrast angiogram shows remarkable tumor stain, but the pulmonary hilar lymphnode cannot be identified (B).

Tissue attenuation correction for emitted gamma-rays was not carried out. The percentage uptake of the whole liver tumor was difficult to calculate because several lesions were multicentric. Instead, the tumor/liver (T/L) ratio was calculated as counts of the tumor divided by counts of the liver parenchyma by means of the same sized ROI.

The washout rates from tumors and normal tissue at 30 and 60 minutes for counts of 1–2 minutes were calculated with corrections for background radioactivity and physical decay. Under curve analysis, a ROI of a contralateral normal lung, or a heart, was regarded as a ROI of background radioactivity in the BAI and HAI studies, respectively.

The tumor delineation of  $^{123}\text{I}$ -IMP infused into the hepatic artery was compared with the tumor stain in the conventional contrast angiography.

Statistical analysis was performed by Student's t-test.

## RESULTS

### *Pulmonary neoplasms*

$^{123}\text{I}$ -IMP infused into the bronchial artery was distributed

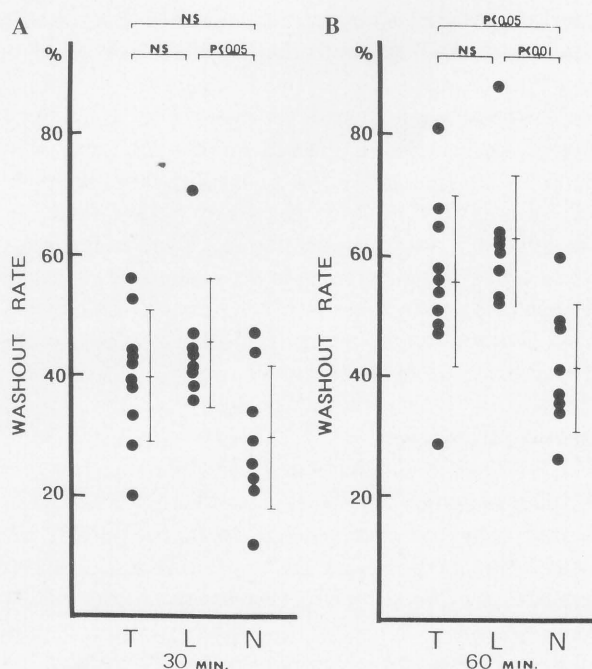


**Fig. 2** The washout rate of  $^{123}\text{I}$ -IMP introduced into bronchial artery for tumor (T), lymphnode (L) and normal area (N) at 30 (A) and 60 (B) minutes post-injection.

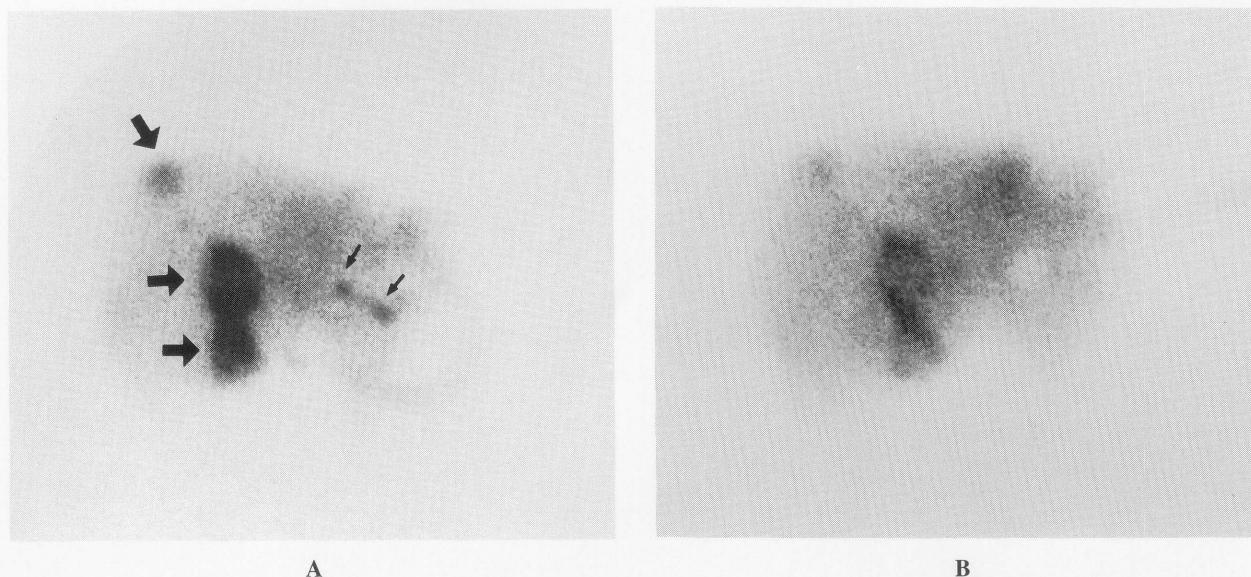


**Fig. 3** A 45-year-old female with multiple metastatic carcinoma from the colon in the right lobe of the liver and previous cholecystectomy. Intensity of  $^{123}\text{I}$ -IMP(A) in the metastatic lesions in the vicinity of porta hepatis and hepatic dome (arrows) in the 3–6 minutes image is higher than that of  $^{99\text{m}}\text{Tc}$ -MAA (B) on right anterior oblique view. Small arrows indicate focal area of activity at subcutaneous reservoir and catheter.

not only in the pulmonary cancer and lymph nodes, but also in normal tissue along the bronchial and intercostal arterial distribution and the mediastinum (Fig. 1).

In the investigation of the percentage uptake of the whole lung and tumor in 11 cases of primary lung carcinoma, the mean value for the whole lung was  $40.6 \pm 9.2\%$ , and that for the tumor was  $14.7 \pm 5.7\%$ . In one case of metastatic breast carcinoma approximately 2 cm in diameter, the percentage uptake of the whole lung was 86.3% and no  $^{123}\text{I}$ -IMP accumulation in the tumor could be detected.

The mean washout rates for  $^{123}\text{I}$ -IMP in 10 tumors, 8 lymph nodes, and 8 normal pulmonary areas were  $39.6 \pm 10.8$ ,  $45.1 \pm 11.0$  and  $29.4 \pm 11.8\%$ , respectively, at 30 minutes; and  $55.6 \pm 14.2$ ,  $62.8 \pm 11.0$  and  $41.4 \pm 10.6\%$  at 60 minutes (Fig. 2). There were statistically significant differences in the washout rate between lymph nodes and normal tissues at 30 and 60 minutes, and also between tumors and normal tissues at 60 minutes ( $p < 0.05$ , 0.01, and 0.05 respectively).

#### Hepatic neoplasms

$^{123}\text{I}$ -IMP was accumulated in the liver parenchyma, gall bladder and tumor. For the cases in which the catheter tip was set at the celiac artery, accumulation of  $^{123}\text{I}$ -IMP was also seen in the spleen and gastrointestinal tract.  $^{123}\text{I}$ -IMP uptake in the liver parenchyma and tumor decreased with time. The splenic uptake of  $^{123}\text{I}$ -IMP decreased with time, and  $^{123}\text{I}$ -IMP in the spleen moved into the liver via the portal vein.

With respect to the comparison of  $^{123}\text{I}$ -IMP studies with  $^{99\text{m}}\text{Tc}$ -MAA studies in 9 patients, the distribution of  $^{123}\text{I}$ -

**Table 2** Count ratio of hepatic tumor to hepatic parenchyma of  $^{123}\text{I}$ -IMP introduced into hepatic artery

	No. of patients	2 min.	30 min.	60 min.
HCC	5	$2.1 \pm 0.7$	$1.8 \pm 0.8$	$1.6 \pm 0.7$
MT	6	$1.4 \pm 0.7$	$1.1 \pm 0.7$	$1.1 \pm 0.7$

HCC: hepatocellular carcinoma

MT: metastatic carcinoma of the liver

IMP was the same as that of  $^{99\text{m}}\text{Tc}$ -MAA in 5 patients and it was different from that of  $^{99\text{m}}\text{Tc}$ -MAA in the rest. However, in the former cases, the intensity of  $^{123}\text{I}$ -IMP activity in the tumor was higher than that of  $^{99\text{m}}\text{Tc}$ -MAA in 2 cases (Fig. 3). In the latter cases, the distribution of  $^{123}\text{I}$ -IMP in the peripheral liver parenchyma was more homogeneous and was better visualized than that of  $^{99\text{m}}\text{Tc}$ -MAA.

The mean percentage uptake in the whole liver was  $40.2 \pm 18.2\%$  in 7 cases in which the catheter tip was set in the right hepatic artery. In 6 cases in the proper hepatic artery, in 3 cases in the common hepatic artery, and in 3 cases in the celiac artery, the mean percentage uptake in the whole liver was  $51.2 \pm 7.2\%$ ,  $41.8 \pm 15.9\%$  and  $16.1 \pm 2.5\%$ , respectively.

The mean T/L ratio in 5 out of 7 HCCs was  $2.11 \pm 0.69$  at 2 minutes,  $1.80 \pm 0.78$  at 30 minutes and  $1.55 \pm 0.67$  at 60 minutes. In the 2 cases excluded from the evaluation, a ROI could not be assigned because the gamma camera was incorrectly positioned. The mean T/L ratio of 6 out of 10 cases of metastatic liver tumors was  $1.37 \pm 0.70$  at 2 minutes and  $1.08 \pm 0.65$  and  $1.09 \pm 0.67$  at 30 and 60 minutes (Table 2). There was no statistically significant difference between the mean T/L ratio of the HCC and the

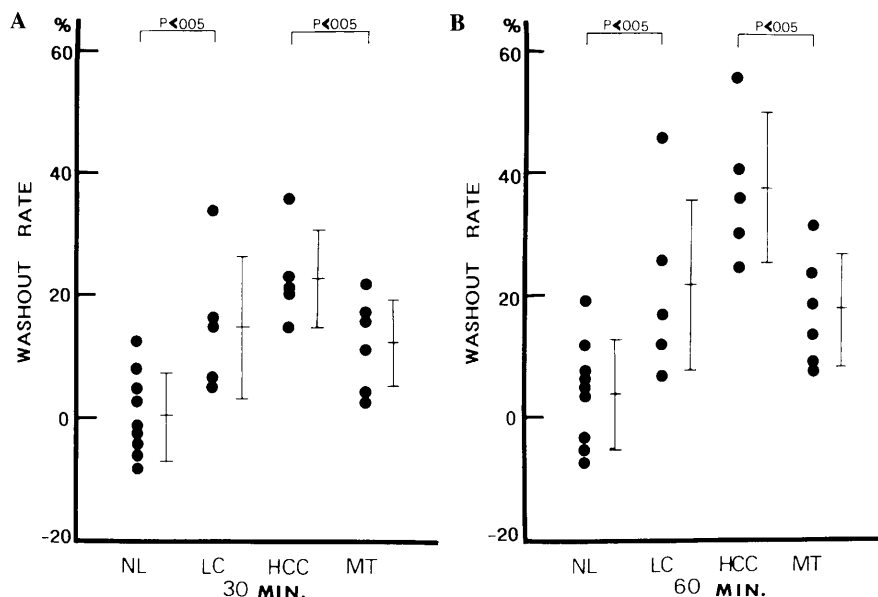


**Fig. 4** The washout rate of  $^{123}\text{I}$ -IMP introduced into hepatic artery for normal liver (NL), liver cirrhosis (LC), hepatocellular carcinoma (HCC) and metastatic carcinoma (MT) at 30 minutes (A) and 60 minutes (B).

metastatic tumor at each time period. In 2 of the 4 cases excluded, the tumors were too small to assign a ROI and in the other 2 cases tumors could not be detected.

The mean washout rate at 30 minutes after the administration of  $^{123}\text{I}$ -IMP was  $0.7 \pm 6.7\%$  from normal liver parenchyma in 9 cases,  $15.2 \pm 11.6\%$  from liver cirrhosis in 5 cases,  $23.2 \pm 7.8\%$  from HCC in 5 cases, and  $12.2 \pm 7.6\%$  from metastatic tumors in 6 cases. The mean washout rate at 60 minutes was  $4.2 \pm 8.3\%$ ,  $21.6 \pm 15.3\%$ ,  $37.6 \pm 11.9\%$  and  $17.7 \pm 9.3\%$ , respectively (Fig. 4). The mean washout rate from liver cirrhosis was faster than that from normal liver parenchyma ( $p < 0.05$ ), and the mean washout rate from HCC was faster than from metastatic tumors at both 30 and 60 minutes ( $p < 0.05$ ).

The tumor uptake of  $^{123}\text{I}$ -IMP in the initial images was compared with the tumor stain in contrast angiograms in 19 patients. Two cases were positive for  $^{123}\text{I}$ -IMP and negative for contrast angiograms, whereas 3 cases were negative for  $^{123}\text{I}$ -IMP and positive for contrast angiogram. In the other 14 cases, the findings of  $^{123}\text{I}$ -IMP scintigraphy were similar to those of the contrast angiography.

## DISCUSSION

$^{123}\text{I}$ -IMP infused into the bronchial or hepatic arteries accumulated in the normal and malignant tissues supplied by those arteries, and the uptake of  $^{123}\text{I}$ -IMP in the tissue decreased with time. Comparing the behavior of  $^{99\text{m}}\text{Tc}$ -MAA and  $^{123}\text{I}$ -IMP infused into the hepatic artery in 9 patients, 4 cases showed different distribution patterns and 2 cases showed different intensities of radionuclide activity in the tumor. Among the former cases, there were 2 cases in which  $^{99\text{m}}\text{Tc}$ -MAA was accumulated only in the

region of the catheter tip, but  $^{123}\text{I}$ -IMP was distributed in both the region of the catheter tip and the liver parenchyma, then  $^{123}\text{I}$ -IMP in the catheter tip moved into the liver parenchyma and the tumor with time. Partial or complete hepatic arterial thrombosis and catheter thrombosis have been reported as the major causes of unsatisfactory perfusion after surgical placement for hepatic chemotherapy.<sup>21-23</sup> From this point of view, there is the possibility that stenosis of the catheter tip due to a thrombus or arterial thrombosis adjacent to the catheter might have been overestimated in the  $^{99\text{m}}\text{Tc}$ -MAA study. In the other 2 cases, the left lobe of the liver was not visualized in  $^{99\text{m}}\text{Tc}$ -MAA scintigraphy but it was seen in  $^{123}\text{I}$ -IMP scintigraphy. The occurrence of laminar flow in the hepatic artery, which may result in poor mixing of the infusate and the blood, might explain these findings.<sup>22-25</sup> The distribution of  $^{99\text{m}}\text{Tc}$ -MAA might be influenced by arterial flow and inadequate mixing in the blood because of its larger molecular weight than that of  $^{123}\text{I}$ -IMP.

The mean percentage uptake of the whole lungs and tumor in primary pulmonary cancer patients, to the total administration dose of  $^{123}\text{I}$ -IMP, was  $40.6 \pm 9.2\%$  and  $14.7 \pm 5.7\%$ . That of the whole liver was about 50% or less. One reason for the low percentage uptake might be calculating without tissue attenuation correction. In addition, the following reasons are also possible: anastomosis of the bronchial artery and pulmonary artery via the capillary bed around the bronchial wall in normal lung, a bronchial-pulmonary shunt as a pre-capillary shunt around the tumor, and a hepatic arterial-venous or arterial-portal shunt.<sup>23,26,27</sup> In these contexts, the percentage uptake of  $^{99\text{m}}\text{Tc}$ -MAA might be overestimated because capillary blockade may happen before an arterial-venous shunt.



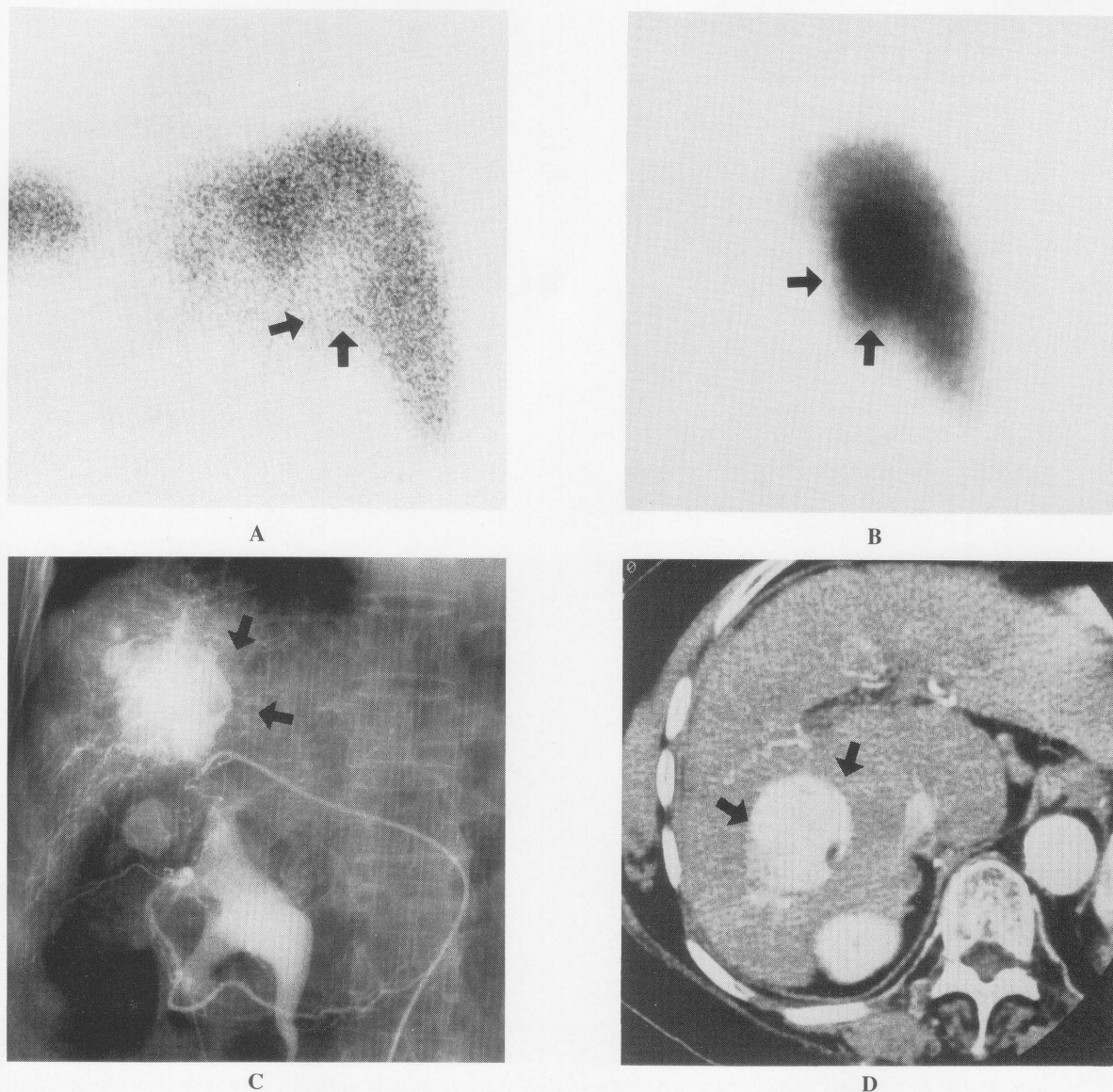


**Fig. 5** A 65-year-old female with hepatocellular carcinoma.  $^{99m}\text{Tc-Sa}$  colloid scintigram of posterior view shows photon deficiency area (arrows) in the right lobe of the liver (A). The 0–3 minutes posterior image with  $^{123}\text{I-IMP}$  demonstrates intense uptake (arrows) in the lesion of the liver (B). Hepatic contrast angiogram (C) and early phase of CT with bolus injection of contrast material (D) shows strong homogeneous tumor stain (arrows).

From the results of this study, the mean T/L ratio of HCC to liver parenchyma, at 2 minutes after the administration of  $^{123}\text{I-IMP}$  into the hepatic artery, was  $2.1 \pm 0.7$ . The case in Figure 5, in which the catheter tip was placed in the right hepatic artery, showed a T/L ratio of 2.26 at 2 minutes. Based on this result, it was surmised that the concentration of chemotherapeutic agent accumulated in the HCC might be more than two times that of the surrounding liver parenchyma. Nakajo et al. reported that the T/L count ratios in HCC were 1.9 to 3.7 by SPECT 2 hours after the arterial infusion of iodine-131-labeled lipiodol and these count ratios corresponded to 7.5–21 in the T/L concentration ratio. These count and concentration ratios were interconnected by an experimental study

by SPECT using the liver, tumor and body phantoms.<sup>28</sup> On the other hand, Raoul et al. noted that the T/L ratio in 23 cases of HCC was  $4.3 \pm 2.6$  by planar scintigrams 24 hours after the arterial infusion of iodine-131-labeled lipiodol ultra-fluid.<sup>29</sup> In patients with hepatic metastases, the mean T/L ratio was  $1.4 \pm 0.7$  at 2 minutes after the administration of  $^{123}\text{I-IMP}$ . Sigurdson et al. mentioned that the T/L ratio in the cases of colorectal hepatic metastases was  $0.78 \pm 2.10$  obtained by planar scintigrams with  $^{99m}\text{Tc-MAA}$  and that after hepatic arterial infusion of  $1 \mu\text{Ci/kg}$   $^3\text{H-fluorodeoxyuridine}$ , the mean tumor uptake of the drug was  $12.4 \pm 12.2 \text{ nmol/g tissue}$ , compared with a mean hepatic level of  $23.9 \pm 11.4 \text{ nmol/g}$ .<sup>11</sup> In both colorectal and carcinoid tumors in the liver, Gyves et al.

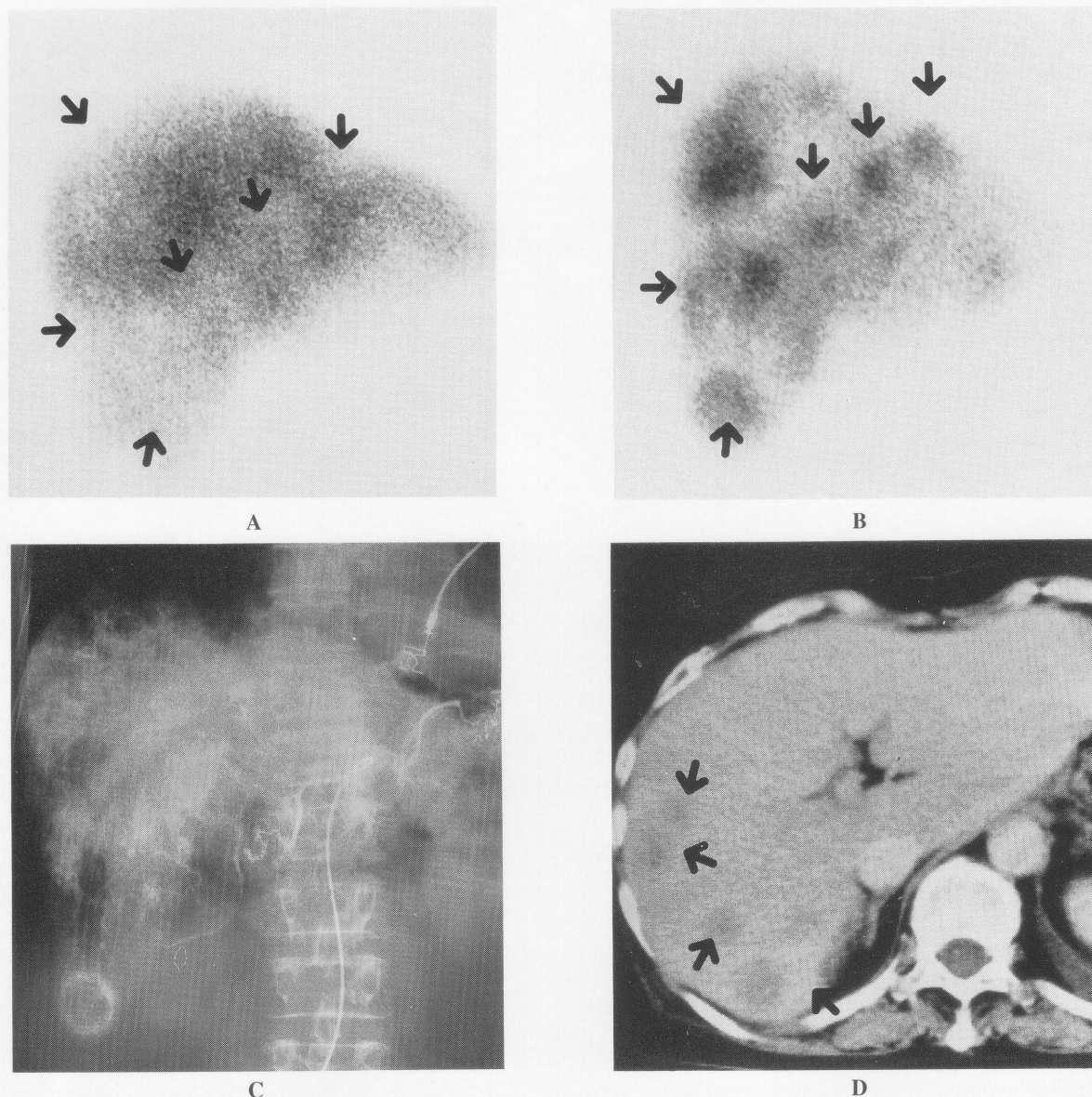


**Fig. 6** A 63-year-old female with multiple metastatic tumor from the stomach.  $^{99m}\text{Tc}$ -Sn colloid scintigram shows multiple photon deficient areas (arrows) on the right anterior oblique view (A). The 0–3 minutes right anterior oblique image with  $^{123}\text{I}$ -IMP introduced into hepatic artery shows multiple nodular uptake (arrows) corresponding to metastatic lesions (B). Hepatic contrast angiogram shows heterogeneous tumor stain in the right lobe of the liver (C). Contrast enhanced CT demonstrates multiple low densities (arrows) with ill-circumscribed tumor margin (D).

demonstrated that the T/L ratio was approximately 3.0 by SPECT with  $^{99m}\text{Tc}$ -MAA.<sup>30</sup>

The washout rate from pulmonary cancers and lymph nodes was faster than that from the normal lung tissue. The slower washout from the normal lung tissue may be due to gradual accumulation and slow release of  $^{123}\text{I}$ -IMP in the lung after systemic circulation of  $^{123}\text{I}$ -IMP. A high lung uptake of  $^{123}\text{I}$ -IMP has been reported and  $^{123}\text{I}$ -IMP is bound to the receptor of the endothelial cell membrane in the pulmonary capillaries.<sup>31,32</sup> In the study of pulmonary cancer with intravenous administration of  $^{123}\text{I}$ -IMP, impaired uptake of  $^{123}\text{I}$ -IMP in the lesion was demon-

strated.<sup>33–35</sup> The washout rate from liver cirrhosis was faster than normal liver parenchyma. This is assumed to be due to a decrease in the cellularity of the liver parenchyma in liver cirrhosis. And the washout rate from HCC was faster than from metastatic cancer. This difference may be due to high blood perfusion in HCC. Also, the effect of the recirculation of  $^{123}\text{I}$ -IMP, the effect of amphetamine derivatives, or the environment of the cells including pH must be taken into consideration.

In the comparison between tumor stain in hepatic contrast angiogram and the tumor uptake of  $^{123}\text{I}$ -IMP, the  $^{123}\text{I}$ -IMP study showed better visualization of the tumors

compared than in contrast angiography in 2 of 19 cases (Fig. 6). Those two cases were one metastatic cancer from the colon and one regenerative nodule of liver cirrhosis. Similar findings are reported in another  $^{99m}\text{Tc}$ -MAA study.<sup>36</sup> On the other hand, in 3 cases (2 HCCs and one metastatic cancer from the colon), no accumulation of  $^{123}\text{I}$ -IMP was detected in spite of a positive tumor stain in contrast angiogram. This is because there was minimum peripheral tumor stain with a central hypovascular area in an angiogram in one case, and the position for scintigraphy was not suitable in the other case.

$^{123}\text{I}$ -IMP accumulated in the hepatic and pulmonary tumors as well as those of parenchyma through the catheter which was placed in the bronchial or hepatic arteries.  $^{123}\text{I}$ -IMP can be used as an intra-arterial imaging agent to estimate the arterial blood supply to the organs with neoplasms and possibly intracellular distribution of chemotherapeutic agents when they are intra-arterially administered.

## ACKNOWLEDGMENTS

I would like to thank M. Furudate, M.D. and K. Itoh, M.D. from Hokkaido University and D. Spigos, M.D. from Ohio State University Hospital (Columbus, Ohio) for their valuable comments, and H. Suzuki, M. Tokita, and S. Kinouchi of the Nuclear Medicine Section of Sapporo City General Hospital for their help and technical support.

## REFERENCES

1. Diksic M, Sako K, Feindel W, Kato A, Yamamoto YL, Farrokhzad S, et al. Pharmacokinetics of positron-labeled 1,3-Bis(2-chloroethyl)nitrosourea in human brain tumors using positron emission tomography. *Cancer Res* 44: 3120–3124, 1984.
2. Tyler JL, Yamamoto YL, Diksic M, Theron J, Villemure JG, Worthington C, et al. Pharmacokinetics of superselective intra-arterial and intravenous [ $^{11}\text{C}$ ]BCNU evaluated by PET. *J Nucl Med* 27: 775–780, 1986.
3. Ginos JZ, Cooper AL, Dhawan V, Lai JCK, Strother SC, Alcock N, et al. [ $^{13}\text{N}$ ]Cisplatin PET to assess pharmacokinetics of intra-arterial versus intravenous chemotherapy for malignant brain tumors. *J Nucl Med* 28: 1844–1852, 1987.
4. Kim EE, Haynie T. Role of nuclear medicine in chemotherapy of malignant lesions. *Semin Nucl Med* 15: 12–20, 1985.
5. Yang PJ, Thrall JH, Ensminger WD, Niederhuber JE, Gyves JW, Tuscan M, et al. Perfusion Scintigraphy ( $\text{Tc-}^{99m}\text{MAA}$ ) during surgery for placement of chemotherapy catheter in hepatic artery: concise communication. *J Nucl Med* 23: 1066–1069, 1982.
6. Bledin AG, Kantarjian HM, Kim EE, Wallace S, Chuang VP, Patt YZ, et al.  $^{99m}\text{Tc}$ -labeled macroaggregated albumin in intrahepatic arterial chemotherapy. *Am J Roentgenol* 139: 711–715, 1982.
7. Rodari A, Bonfanti G, Garbagnati F, Marolda R, Milella M, Buraggi GL. Microsphere angiography in hepatic artery

- infusion for cancer. *Eur J Nucl Med* 6: 473–476, 1981.
8. Sasaki Y, Imaoka S, Hasegawa Y, Nakano S, Ishikawa O, Ohigashi H, et al. Distribution of arterial blood flow in human hepatic cancer during chemotherapy-examination by short-lived  $^{81m}\text{Kr}$ . *Surgery* 97: 409–413, 1985.
9. Sigurdson ER, Ridge JA, Daly JM. Fluorodeoxyuridine uptake by human colorectal hepatic metastases after hepatic artery infusion. *Surgery* 100: 285–291, 1986.
10. Ridge JA, Sigurdson ER, Daly JM. Distribution of fluorodeoxyuridine uptake in the liver and colorectal hepatic metastases of human beings after arterial infusion. *Surg Gynecol Obstet* 164: 319–323, 1987.
11. Sigurdson ER, Ridge JA, Kemeny N, Daly JM. Tumor and liver drug uptake following hepatic artery and portal vein infusion. *J Clin Oncol* 5: 1836–1840, 1987.
12. Kaplan WD, Ensminger WD, Come SE, Smith EH, D'Orsi CJ, Levin DC, et al. Radionuclide angiography to predict patient response to hepatic artery chemotherapy. *Cancer Treat Rep* 64: 1217–1222, 1980.
13. Daly JM, Butler J, Kemeny N, Yeh SDJ, Ridge JA, Botet J, et al. Predicting tumor response in patients with colorectal hepatic metastases. *Ann Surg* 202: 384–393, 1985.
14. Lassen NA, Henriksen L, Holm S, Barry DL, Paulson OB, Vorstrup S, et al. Cerebral blood flow tomography: Xenon-133 compared with isopropylamphetamine Iodine 123 concise communication. *J Nucl Med* 24: 17–21, 1983.
15. Drayer B, Jaszczak R, Friedman A, Albright R, Kung H, Greer K, et al. *In vivo* quantitation of regional cerebral blood flow in glioma and cerebral infarction: validation of the HIPDM-SPECT method. *AJNR* 4: 572–576, 1983.
16. Winchell HS, Baldwin RM, Lin TH. Development of I-123-labeled amines for brain studies: Localization of I-123 iodophenylalkyl amines in rat brain. *J Nucl Med* 21: 940–946, 1980.
17. Winchell HS, Horst WD, Braun L, Oldendorf WH, Hattner R, Parker H, et al. N-isopropyl-[ $^{123}\text{I}$ ]p-iodoamphetamine: Single-pass brain uptake and washout; Binding to brain synaptosomes; and localization in dog and monkey brain. *J Nucl Med* 21: 947–952, 1980.
18. Kuhl DE, Barrio JR, Huang SC, Selin C, Ackermann RF, Lear JJ, et al. Quantifying local cerebral blood flow by N-isopropyl-p-[ $^{123}\text{I}$ ]iodoamphetamine (IMP) tomography. *J Nucl Med* 23: 196–203, 1982.
19. Holman BL, Lee RGL, Hill TC, Lovett RD, Lister-James J. A comparison of two cerebral perfusion tracers, N-isopropyl I-123 p-iodoamphetamine and I-123 HIPDM, in the human. *J Nucl Med* 25: 25–30, 1984.
20. Moretti JL, Cinotti L, Cesaro P, Defer G, Joulin Y, Sergeant A, et al. Amines for brain tomoscintigraphy. *Nucl Med Commun* 8: 581–595, 1987.
21. Stagg RJ, Lewis BJ, Friedman MA, Ignoffo RJ, Hohn DC. Hepatic arterial chemotherapy for colorectal cancer metastatic to the liver. *Ann Intern Med* 100: 736–743, 1984.
22. Andrews JC, Williams DM, Cho KJ, Knol JA, Wahl RL, Ensminger WD. Unsatisfactory hepatic perfusion after placement of an implanted pump and catheter system: angiographic correlation. *Radiology* 173: 779–781, 1989.
23. Cho KJ, Andrews JC, Williams DM, Doenz F, Guy GE. Hepatic arterial chemotherapy: role of angiography. *Radiology* 173: 783–791, 1989.
24. Charnsangavej C, Carrasco CH, Wallace S, Richli W,



- Haynie TP. Hepatic arterial flow distribution with hepatic neoplasms: significance in infusion chemotherapy. *Radiology* 165: 71–73, 1987.
25. Lutz RJ, Miller DL. Mixing studies during hepatic arterial infusion in an *in vitro* model. *Cancer* 62: 1066–1073, 1988.
  26. Bookstein JJ, Cho KJ, Davis GB, Dail D. Arteriportal communications: observations and hypotheses concerning transsinusoidal and transvasal types. *Radiology* 142: 581–590, 1982.
  27. Fishman AP, Fisher AB, Geiger SR. The respiratory system. *Handbook of Physiology*. Vol. 1. Sec. 3. Bethesda: American physiological society, 1985.
  28. Nakajo M, Kobayashi H, Shimabukuro K, Shirono K, Sakata H, Taguchi M, et al. Biodistribution and *in vivo* kinetics of iodine-131 lipiodol infused via the hepatic artery of patients with hepatic cancer. *J Nucl Med* 29: 1066–1077, 1988.
  29. Raoul JL, Bourguet P, Bretagne JF, Duvauferrier R, Coornaert S, Darnault P, et al. Hepatic artery injection of I-131-labeled lipiodol. *Radiology* 168: 541–545, 1988.
  30. Gyves JW, Ziessman HA, Ensminger WD, Thrall JH, Niederhuber JE, Keyes JW. Definition of hepatic tumor microcirculation by single photon emission computerized tomography (SPECT). *J Nucl Med* 25: 972–977, 1984.
  31. Rahimian J, Glass EC, Touya JJ, Akber SF, Graham LS, Bennett LR. Measurement of metabolic extraction of tracers in the lung using a multiple indicator dilution technique. *J Nucl Med* 25: 31–37, 1984.
  32. Touya JJ, Rahimian J, Corbus HF, Grubbs DE, Savala KM, Glass EC, et al. The lung as a metabolic organ. *Semin Nucl Med* 16: 296–305, 1986.
  33. Nakajo M, Shimada J, Shimozone M, Uchiyama N, Hiraki Y, Shinohara S. Serial lung imaging with <sup>123</sup>I-IMP in localized pulmonary lesions. *KAKU IGAKU (Jpn J Nucl Med)* 25: 441–450, 1988.
  34. Suga K, Matsumoto T, Nakanishi T, Yokoyama T, Tanaka K, Nakamura H, et al. Clinical study on the mechanism of abnormal accumulation in lung scanning with N-isopropyl-p-<sup>123</sup>I-iodoamphetamine (<sup>123</sup>I-IMP). *KAKU IGAKU (Jpn J Nucl Med)* 25: 625–631, 1988.
  35. Kosuda S, Kawahara S, Tamura K, Ishikawa N, Ono A, Kubo A, et al. N-isopropyl-p-[I-123]iodoamphetamine lung imaging in a patient with chronic pulmonary thromboembolism. *Clin Nucl Med* 14: 756–758, 1989.
  36. Herba MJ, Illescas FF, Thirlwell MP, Boos GJ, Rosenthal L, Atri M, et al. Hepatic malignancies: improved treatment with intraarterial Y-90. *Radiology* 169: 311–314, 1988.